Mice with Disrupted Type I Protein Kinase A Anchoring in T Cells Resist Retrovirus-Induced Immunodeficiency

Randi Mosenden, Pratibha Singh, Isabelle Cornez, Mikael Heglind, Anja Ruppelt, Michel Moutschen, Sven Enerbäck, Souad Rahmouni and Kjetil Taskén

J Immunol 2011;186;5119-5130; Prepublished online 23 March 2011;
doi:10.4049/jimmunol.1100003
http://www.jimmunol.org/content/186/9/5119

The Journal of Immunology is published twice each month by
The American Association of Immunologists, Inc.,
9650 Rockville Pike, Bethesda, MD 20814-3994.

Print ISSN: 0022-1767 Online ISSN: 1550-6606.

Mice with Disrupted Type I Protein Kinase A Anchoring in T Cells Resist Retrovirus-Induced Immunodeficiency

Randi Mosenden,*,†,[1] Pratibha Singh,‡,[1] Isabelle Cornez,*,† Mikael Heglind,§ Anja Ruppelt,*,[2] Michel Moutschen,‡ Sven Enerbäck,§ Souad Rahmouni,‡ and Kjetil Taskén*,†

Type I protein kinase A (PKA) is targeted to the TCR-proximal signaling machinery by the A-kinase anchoring protein ezrin and negatively regulates T cell immune function through activation of the C-terminal Src kinase. RI anchoring disruptor (RIAD) is a high-affinity competitor peptide that specifically displaces type I PKA from A-kinase anchoring proteins. In this study, we disrupted type I PKA anchoring in peripheral T cells by expressing a soluble ezrin fragment with RIAD inserted in place of the endogenous A-kinase binding domain under the *lck* distal promoter in mice. Peripheral T cells from mice expressing the RIAD fusion protein (RIAD-transgenic mice) displayed augmented basal and TCR-activated signaling, enhanced T cell responsiveness assessed as IL-2 secretion, and reduced sensitivity to PGE_2- and cAMP-mediated inhibition of T cell function. Hyperactivation of the cAMP–type I PKA pathway is involved in the T cell dysfunction of HIV infection, as well as murine AIDS, a disease model induced by infection of C57BL/6 mice with LP-BM5, a mixture of attenuated murine leukemia viruses. LP-BM5–infected RIAD-transgenic mice resist progression of murine AIDS and have improved viral control. This underscores the cAMP–type I PKA pathway in T cells as a putative target for therapeutic intervention in immunodeficiency diseases. ***The Journal of Immunology*****, 2011, 186: 5119–5130.**

T cells are key players in the adaptive immune system, protecting us against infectious agents and cancer. Exaggerated T cell activity, in contrast, may lead to autoimmune disease. It is therefore essential that the T cell immune response is tightly regulated. cAMP negatively regulates T cell immune function through activation of protein kinase A (PKA) (1). Type I PKA (regulatory subunit $[R]I\alpha_2$ catalytic subunit $[C]_2$) is the predominant PKA isoform in T cells (2, 3). Furthermore, whereas type II PKA ($RII\alpha_2C_2$) is located at the centrosome, type I PKA is anchored close to the TCR (4) in lipid rafts, where it enhances the activity of C-terminal Src kinase (Csk) by phosphorylation on S364 (1). Csk is recruited to lipid rafts through interaction with the phosphorylated transmembrane adaptor protein phosphoprotein associated with glycosphingolipid-enriched microdomains (PAG) (5, 6) and represents the most TCR-proximal PKA substrate in T cells. Activated Csk negatively regulates Src family tyrosine kinase activity (7, 8) and thereby downregulates T cell activation.

PKA is assembled into multiprotein signaling complexes with its selected substrates at particular subcellular locations by A-kinase anchoring proteins (AKAPs), scaffold proteins that provide specificity in cAMP signaling. We have identified ezrin as the functionally important AKAP for type I PKA in T cell lipid rafts (9). Ezrin is a cytoskeletal adaptor protein that provides a link between the actin cytoskeleton and the cell membrane, and thereby governs membrane structure and organization. Ezrin has an N-terminal band 4.1 ezrin/radixin/moesin domain through which it interacts with PAG via ezrin/radixin/moesin-binding phosphoprotein of 50 kDa (EBP50) (10–12), a central α-helical region spanning the A-kinase binding domain (AKB) (9) and a C-terminal actin binding domain (13). Thus, type I PKA is targeted to Csk via the ezrin–EBP50–PAG scaffold complex.

Murine AIDS (MAIDS) occurs postinfection of C57BL/6 mice with LP-BM5, a complex mixture of murine leukemia viruses (MuLVs) that includes replication-competent ecotropic-inducing and mink cell focus-inducing, and replication-defective (BM5def) MuLVs (14, 15). The disease is characterized by initial lymphoproliferation affecting both T and B cells, hypergammaglobulinemia, development of splenomegaly and lymphadenopathy, followed by severe T cell anergy and immunodeficiency, leading to increased susceptibility to opportunistic infections, neoplasms, and ultimately death at 16–24 wk postinfection. Hyperactivation of the cAMP–type I PKA pathway is involved in the T cell dysfunction in MAIDS (16, 17), as well as HIV infection (18). Blocking this pathway partially restores T cell function in vitro in MAIDS (16, 17) and in HIV infection (18). Thus, although the MAIDS model is quite distinct from the virology and biology implicated in HIV infection, it is a suitable model for

*The Biotechnology Center of Oslo, University of Oslo, N-0317 Oslo, Norway; †Center for Molecular Medicine Norway, Nordic European Molecular Biology Laboratory Partnership, University of Oslo, N-0318 Oslo, Norway; ‡Laboratory of Immunology and Infectious Diseases, Interdisciplinary Cluster for Applied Genoproteomics, University of Liège, 4000 Liège-Sart Tilman, Belgium; and §Department of Medical and Clinical Genetics, Institute of Biomedicine, Sahlgrenska Academy, University of Gothenburg, SE-405 30 Gothenburg, Sweden

[1]R.M. and P.S. contributed equally to this work.

[2]Current address: Department of Biochemistry, Institute of Basic Medical Sciences, University of Oslo, Oslo, Norway.

Received for publication January 14, 2011. Accepted for publication February 25, 2011.

This work was supported by grants from the Norwegian Functional Genomics Programme, the Research Council of Norway, the Norwegian Cancer Society, the Novo Nordic Foundation Committee, the European Union (Grant 037189, thera-cAMP), the Belgian National Fund for Scientific Research, and Télévie.

Address correspondence and reprint requests to Dr. Kjetil Taskén, The Biotechnology Center, University of Oslo, P.O. Box 1125 Blindern, N-0317 Oslo, Norway. E-mail address: kjetil.tasken@biotek.uio.no

Abbreviations used in this article: AKAP, A-kinase anchoring protein; AKB, A-kinase binding domain; Ax, Alexa Fluor; C, catalytic subunit; 8-CPT-cAMP, 8-(4-chlorophenylthio)-cAMP; Csk, C-terminal Src kinase; EBP50, ezrin/radixin/moesin-binding phosphoprotein of 50 kDa; GIGA-R, Interdisciplinary Cluster for Applied Genoproteomics; HA, hemagglutinin; LAT, linker for activation of T cells; Lck, lymphocyte-specific protein-tyrosine kinase; MAIDS, murine AIDS; MuLV, murine leukemia virus; PAG, phosphoprotein associated with glycosphingolipid-enriched microdomains; PD-1, programmed death 1; PKA, protein kinase A; R, regulatory subunit; RIAD, RI anchoring disruptor; RISR, RI specifier region; Treg, regulatory T cell.

the cAMP- and type I PKA-mediated T cell dysfunction of HIV infection.

We have previously reported the design of the RI anchoring disruptor (RIAD) peptide that specifically displaces type I PKA from lipid rafts and downregulates cAMP-mediated inhibition of primary human T cell function (19). We have also identified an additional PKA-binding determinant, RI specifier region (RISR), upstream of the traditional AKB in the dual-specificity AKAP ezrin. The RISR acts in synergy with the AKB to enhance anchoring of type I PKA (20). In this article, we explore the effects of perturbing the inhibitory cAMP–type I PKA pathway in mouse peripheral T cells by introducing RIAD in the context of a soluble ezrin fragment containing the endogenous RISR under control of the *lck* distal promoter in mice. Peripheral T cells from RIAD-transgenic mice displayed enhanced T cell signaling and responsiveness. Furthermore, peripheral T cells from RIAD-transgenic mice were less sensitive to cAMP-mediated inhibition of T cell immune function. On LP-BM5 infection, the RIAD-transgenic mice showed resistance to development of MAIDS-associated splenomegaly, lymphadenopathy, and T cell anergy, and viral load was also lower. Furthermore, the emergence of MAIDS phenotypic characteristics was dampened.

Materials and Methods

Engineering of the transgene construct and generation of transgenic mice

Nt 934–1236 were PCR-amplified from human ezrin cDNA, introducing new 5′ BamHI and 3′ NheI restriction sites, and fused to an oligonucleotide consisting of the RIAD sequence in frame with a hemagglutinin (HA) epitope tag flanked by 5′ NheI and 3′ BamHI restriction sites. The resulting construction, referred to as the RIAD construct, was verified by sequencing. For mammalian cell expression, a Kozak sequence (21) was engineered in front of the ATG and a stop codon added on insertion into the pFLAG-CMV-5a vector. The RIAD construct was also inserted between the mouse *lck* distal promoter and introns and exons of the human growth hormone gene (included to increase transgene expression) (22, 23) of the pW120 vector (24, 25) to create pW120 w/RIAD.

Vector-derived sequences were removed by restriction digestion and gel purification, and the promoter-open reading frame fragment was used to make RIAD-transgenic mice on a C57BL/6 × CBA background by pronuclear microinjection as described previously (26–28). RIAD-transgenic founder mice were crossed on the C57BL/6 background for up to 10 generations under specific pathogen-free conditions at the animal facility at Department of Medical and Clinical Genetics, Institute of Biomedicine, University of Gothenburg, Gothenburg, Sweden, the National Lab Animal Center at the Norwegian Institute of Public Health, Oslo, Norway, and the Interdisciplinary Cluster for Applied Genoproteomics (GIGA-R) animal facility at University of Liège, Laboratory of Immunology and Infectious Diseases, Liège-Sart Tilman, Belgium. Mice were weighed before being sacrificed by cervical dislocation. For genotyping, tail or ear biopsies were incubated in 100 μl of 25 mM NaOH and 0.2 mM EDTA at 95˚C for 20 min. After incubation, an equal volume of 40 mM Tris-HCl was added and the solution mixed. PCR genotyping was performed using primers 5′-CCCTCAGGAGACAGGAAGTCAG-3′, 5′-CCTAAGGTGGGAAATGATGGACAG-3′, and 5′-GCAGCATCAACTCCTCCTTCTC-3′, and AccuPrime Pfx Supermix (Invitrogen). Products and DNA sizing ladder (Low DNA Mass Ladder; Invitrogen) were separated by agarose gel electrophoresis and visualized using Gel Star Nucleic Acid Gel Stain (Invitrogen). Animal care was in accordance with national legislation and institutional guidelines. All use of animals has been approved and registered by national animal research authorities.

Cell culture and transient transfections

COS-7 cells were maintained in DMEM GlutaMAX supplemented with 10% FBS, 1 mM sodium pyruvate, 1:100 MEM nonessential amino acids, 100 U/ml penicillin, and 100 μg/ml streptomycin (all from Invitrogen) (complete medium). At 90% confluence, the cells were transfected with 10 μg pFLAG-CMV-5a containing the RIAD construct per 56.7-cm^2 culture dish using FuGENE 6 Transfection Reagent (Roche). After 24 h, the cells were lysed in 50 mM Tris (pH 7.4), 100 mM NaCl, 5 mM EDTA, and 1% Triton X-100 with 50 mM NaF, 10 mM sodium pyrophosphate, 1 mM Na_3VO_4, and 1 mM PMSF (lysis buffer).

Jurkat TAg, a derivative of the human leukemic T cell line Jurkat stably transfected with the SV40 large T Ag (29), was kept at logarithmic growth in RPMI 1640 GlutaMAX (Invitrogen) complete medium. For transfections, 2×10^7 cells in OPTI-MEM (Invitrogen) were mixed with 40–80 μg pW120 w/RIAD in electroporation cuvettes with a 0.4-cm electrode gap (Bio-Rad) and subjected to an electric field of 250 V/cm with 950 μF capacitance. The cells were expanded in RPMI 1640 GlutaMAX complete medium for 20 h before harvest in lysis buffer.

Immunoprecipitations

For immunoprecipitations, COS-7 cell lysates were precleared with mouse γ-globulin (Jackson ImmunoResearch) and protein A/G PLUS-agarose immunoprecipitation reagent (Santa Cruz Biotechnology) at 4˚C for 30 min. The lysates were transferred to new tubes, and Ab against HA (16B12; BioSite), RIα (4D7) (4, 30), or mouse γ-globulin as a control and protein A/G PLUS-agarose immunoprecipitation reagent were added and incubation at 4˚C continued overnight. Subsequently, immune complexes were washed once in lysis buffer and subjected to SDS-PAGE and immunoblotting.

Far Western analyses with radiolabeled R (R overlays)

Jurkat TAg or mouse splenic T cell lysates were subjected to SDS-PAGE and R overlays were conducted as described previously (31), using ^{32}P-labeled recombinant bovine RIα (A98S), substituted to allow autophosphorylation (19, 32), or recombinant mouse RIIα (33). In brief, the membrane with immobilized protein was blocked in 5% nonfat dry milk/0.1% BSA/TBST (blotto). Purified recombinant R (2 μg) was radiolabeled using purified C (1.5 μg) and [γ-^{32}P]ATP (0.05 mCi; PerkinElmer) in 50 mM MOPS (pH 6.8), 50 mM NaCl, 2 mM $MgCl_2$, and 1 mM DTT at 37˚C for 30–45 min, and separated from free [γ-^{32}P]ATP by gel filtration (NICK Column Sephadex G-50; GE Healthcare). Specific activity was quantified by liquid scintillation counting (1600TR Tri-Carb; Packard Instrument). All overlays were performed overnight at room temperature using 1×10^6 cpm/ml TBST. The membrane was washed in TBST five times and signal detected by autoradiography.

Isolation of lipid rafts

Purification of lipid rafts from Jurkat TAg lysates by density gradient centrifugation was performed as described previously (34). The peak raft fractions were pooled and subjected to SDS-PAGE and immunoblotting. Densitometry measurements were done using Quantity One 4.5 (Bio-Rad).

SDS-PAGE and immunoblotting

Immune complexes from immunoprecipitations, cell or tissue lysates, or pooled peak raft fractions were separated by SDS-PAGE and transferred to PVDF membranes by electroblotting. Membranes were blocked in 5% nonfat dry milk/TBST or 3% BSA/TBST for phospho-Ab at room temperature for 1 h, and incubated at 4˚C overnight with primary Ab diluted in 5% nonfat dry milk/TBST or 3% BSA/TBST for phospho-Ab. Ab used were against RIα (20; BD Biosciences), HA (16B12, BioSite or 3F10, Roche), actin (C-11; Santa Cruz Biotechnology), linker for activation of T cells (LAT; Upstate Biotechnology), GAPDH (mAbcam 9484; Abcam), Akt (pT308; Cell Signaling), phosphotyrosine (4G10; Upstate Biotechnology), and Src family (pY416; Cell Signaling). For secondary detection, HRP-conjugated Ab (Jackson ImmunoResearch/GE Healthcare) were used and membranes were developed using SuperSignal West Pico Chemiluminescent Substrate (Pierce)/ECL Detection Reagents (GE Healthcare).

Tissue lysis

Mouse tissues were dissected and transferred to ice-cold 50 mM Tris-HCl (pH 7.4), 150 mM NaCl, 1 mM EDTA, and 1% Triton X-100. Tissues were then homogenized using a Polytron PT-3000 (Kinematica). Homogenates were incubated with slow shaking at 4˚C for 60 min and then centrifuged at 12,000 × *g* at 4˚C for 10 min. Supernatants were transferred to clean tubes. Centrifugation and supernatant collection were repeated until the extracts were clear. Protein concentrations were determined using the Bio-Rad Protein Assay, based on the method of Bradford, and 20 μg protein was loaded in each well.

Isolation of T cells from mouse spleen

Spleens were dissected, weighed, and converted into single-cell suspensions by squeezing through a 100-μm cell strainer (Falcon) in PBS. Erythrocytes were depleted by lysis in hypotonic buffer (RBC Lysing Buffer; Sigma-

Aldrich). The buffer was neutralized with RPMI 1640 GlutaMAX, and splenocytes were resuspended in 0.1% BSA/2 mM EDTA/PBS (pH 7.4) and counted on a Z2 Coulter Particle Count and Size Analyzer (Beckman Coulter). $CD3^+$ T cells were isolated using Dynal Mouse T Cell Negative Isolation Kit (Invitrogen) according to the manufacturer's protocol and counted. When needed, the cells were lysed in lysis buffer.

Immunofluorescence

For immunofluorescence studies, freshly isolated mouse splenic T cells were settled on poly-L-lysine (Sigma-Aldrich)–coated coverslips on ice for 30 min. Capping of the TCR was achieved by incubating cells with 1 μg/ml biotin-conjugated hamster anti-mouse CD3e (145-2C11; BD Biosciences) in 0.1% BSA/PBS on ice for 30 min, followed by transfer to poly (L-lysine)–coated coverslips and incubation with 10 μg/ml streptavidin, Alexa Fluor (Ax) 405 conjugate (Invitrogen) in 0.1% BSA/PBS on ice for 30 min, and then at 37°C for 20 min. The cells were next fixed with 3% PFA/PBS for 30 min, permeabilized with 0.1% NP-40/PBS for 5 min, and then blocked with 2% BSA/0.01% Tween 20/PBS for 30 min. Primary Ab against HA (16B12; BioSite), RIα (4D7), Cα (A-2; Santa Cruz Biotechnology), and RIIα (M-20; Santa Cruz Biotechnology) in 2% BSA/0.01% Tween 20/PBS were added for 30 min. The cells were then incubated with fluorochrome-conjugated secondary Ab (Ax488 goat anti-mouse IgG_1, Ax488/546 goat anti-mouse IgG_{2a}, Ax555 goat anti-rabbit IgG; Invitrogen) in 2% BSA/0.01% Tween 20/PBS for 30 min before being mounted on glass microscope slides using Fluorescent Mounting Medium (DakoCytomation). Confocal microscopy was performed with a Zeiss LSM 510 META confocal microscope with a Plan-Apochromat 63 × 1.4 Oil differential interference contrast objective lens, using laser excitation at 405, 488, and 561 nm. The widths of the emission channels were set such that bleed through across channels was negligible, and pictures were obtained using sequential scanning. Relative colocalization was calculated as total red *and* green (yellow) divided by total red *or* green pixels in each cell using ImageJ software.

Stimulation for phosphostatus analyses

A total of 8×10^7 freshly isolated mouse splenic T cells/ml in RPMI 1640 GlutaMAX were equilibrated at 37°C for 10 min. The cells were then activated by the addition of 1 μg/ml biotin-conjugated hamster anti-mouse CD3e (145-2C11; BD Biosciences) and 1 μg/ml biotin-conjugated rat anti-mouse CD4 (RM4-5; BD Biosciences), followed by cross-linking with 40 μg/ml avidin (Invitrogen) at 37°C for the indicated times. Activation was terminated by transfer to ice and addition of 2× lysis buffer.

Flow cytometry

A total of 1×10^6 freshly isolated mouse splenic T cells were fixed 1:1 in BD Phosflow Fix Buffer I (BD Biosciences) at 37°C for 10 min. The cells were permeabilized in ice-cold BD Phosflow Perm Buffer III (BD Biosciences) and kept at −80°C at least overnight. Subsequently, 0.5×10^6 cells were stained with a mixture of Ab against HA (Ax488-conjugated, 6E2; Cell Signaling), CD8 (allophycocyanin-eFluor 780-conjugated, 53-6.7), FOXP3 (allophycocyanin-conjugated, FJK-16s) (both eBioscience), CD3 (PE-conjugated, 17A2), CD4 (PerCP-conjugated, RM4-5), CD45R (PerCP-conjugated, RA3-6B2), CD11b (allophycocyanin-conjugated, M1/70), and CD25 (PE-conjugated, PC61) (all from BD Biosciences). After labeling at room temperature for 30 min, the cells were resuspended in 1% FBS/0.09% NaN_3/PBS before FACS analysis. Regarding lymph node cells, 1×10^6 freshly isolated cells were blocked with Ab against CD16/CD32 (FcγRIII/II, 2.4G2) for 15 min before labeling with Ab against CD4 (PE-conjugated, GK 1.5 or FITC-conjugated, RM4-5), CD45R (FITC-conjugated, RA3-6B2), CD11b (PE-conjugated, M1/70), CD3 (allophycocyanin-conjugated, 145-2C11), CD90.2 (FITC-conjugated, 30.H12), and CD279 (PE-conjugated, J43) (all from BD Biosciences). Data were acquired on a FACSCanto II flow cytometer (BD Biosciences) equipped with 407-, 488-, and 633-nm lasers. Data were subsequently analyzed using FlowJo software (Tree Star).

Cytokine production assays

Freshly isolated mouse splenic T cells were seeded into 96-well flat-bottom plates at a concentration of 2×10^6 cells/ml in RPMI 1640 GlutaMAX complete medium and incubated with increasing concentrations of 8-(4-chlorophenylthio)-cAMP (8-CPT-cAMP; BioLog Life Science) or PGE_2 (Sigma-Aldrich) at 37°C for 30 min before stimulation with Dynabeads Mouse CD3/CD28 T Cell Expander (Invitrogen) at cell/bead ratio 1:1 at 37°C for 20 h. Cell-free supernatants were harvested and cytokine levels quantified by ELISA (IL-2; R&D Systems) or using a Bio-Plex System (Bio-Rad) and a Bio-Plex Mouse Cytokine Th1/Th2 Panel (Bio-Rad), allowing for the multiplexed detection of mouse IL-4, IL-5, IL-10, IL-12, GM-CSF, IFN-γ, and TNF-α in each sample. The assays were performed in accordance with the manufacturer's instructions. The IC_{50} values, defined as the concentration of 8-CPT-cAMP/PGE_2 needed to inhibit IL-2 production by 50%, were estimated by nonlinear regression analyses using SigmaPlot (SPSS).

Virus

The LP-BM5–producing SC-1/MuLV cell line (AIDS Research and Reference Reagent Program, Division of AIDS, National Institute of Allergy and Infectious Diseases, National Institutes of Health), established by cocultivation of SC-1 cells with mitomycin C-treated cells obtained from the enlarged lymph nodes of a C57BL/6 mouse inoculated with virus harvested from a reticulum cell neoplasm-BM5 stromal cell line established by Haas and Reshef (35), was maintained in accordance with the protocol provided. In brief, SC-1/MuLV cells were grown in DMEM GlutaMAX complete medium, and viruses were extracted from the supernatant of confluent cells and stored in liquid nitrogen.

Induction of MAIDS and isolation of lymph node cells

Six- to 8-wk-old RIAD-transgenic mice and sex-matched wild-type littermates were injected four times i.p. at 1-wk intervals with 0.5 ml viral extract. Age- and sex-matched C57BL/6 control mice were correspondingly injected with 0.5 ml PBS. Eight to 9 wk after the last injection, the mice were sacrificed by cervical dislocation. Spleens and lymph nodes (cervical, mesenteric, inguinal, and axillary) were dissected and weighed. Inguinal and axillary lymph nodes were converted into single-cell suspensions by squeezing through a 100-μm cell strainer (Falcon); lymph node cells were washed three times in RPMI 1640 complete medium and counted on a Thoma cytometer (Mariefeld) after trypan blue (Invitrogen) exclusion.

Proliferation assays

Freshly isolated mouse lymph node cells were seeded into 96-well flat-bottom plates at a concentration of 1×10^6 cells/ml in RPMI 1640 supplemented with 10% FBS, 10^{-5} M 2-ME, 1 mM sodium pyruvate, 1:100 MEM nonessential amino acids, 60 U/ml penicillin, and 60 μg/ml streptomycin (all from Invitrogen) and stimulated with 5 μg/ml CD3 Ab (145-2C11; BD Biosciences) and/or 50 U/ml IL-2 (Roche) at 37°C for 72 h. A total of 0.4 μCi [^{3}H]thymidine (PerkinElmer) was included for the last 4 h. Cells were harvested (Filter Mate; PerkinElmer) and proliferation was quantified using TopCount NXT Microplate Scintillation and Luminescence Counter (PerkinElmer).

RNA extraction, reverse transcription, and quantitative real-time PCR

RNA was extracted from mouse lymph nodes using TRIzol, reversely transcribed (1 μg) using Expand Reverse Transcriptase, and quantitative real-time PCR was performed using 2 μl diluted cDNA (1:1000), primers 5′-CCTCCTAAGTCCCGGGTTCTC-3′ and 5′-CGGCCGCCTCTTCTTA-ACT-3′ for BM5def and 5′-CACCCCACTGAGACTGATACA-3′ and 5′-TGATGCTTGATCACATGTCTCG-3′ for B2M and SYBR Green PCR Master Mix (all from Roche) in accordance with the manufacturer's instructions. All PCR was performed on LightCycler Systems for real-time PCR (Roche).

Statistics

Graphs were made in SigmaPlot 8.0 (SPSS). Statistical analyses were performed using the Mann–Whitney *U* test, conducted in SPSS 16.0 for Windows. Results are given as medians and 25th percentiles unless otherwise stated. The two-sided *p* values were considered statistically significant at $p < 0.05$.

Results

Engineering of T cell-specific disruption of type I PKA anchoring

Given the demonstrated role of lipid raft-targeted type I PKA in cAMP-mediated modulation of T cell immune function (1, 9), we wanted to explore the outcome of competing the anchoring of type I PKA to T cell lipid rafts by its AKAP ezrin in a physiological context. We engineered a construct comprising aa 312–413 from the α-helical region of ezrin (including the endogenous RISR)

with the high-affinity RI-specific RIAD inserted in the position of the endogenous AKB and a C-terminal HA epitope tag (see boxed areas in Fig. 1*B*). To examine the function of RIAD in the context of the soluble ezrin fragment containing the endogenous RISR, COS-7 cells expressing this RIAD fusion protein under the CMV promoter were lysed and subjected to immunoprecipitations with Ab to the HA epitope and RIα (Fig. 1*A*). In such experiments, endogenous RI coimmunoprecipitated with the RIAD fusion protein and vice versa. Control immunoprecipitations with mouse IgG were negative (data not shown). Thus, the RIAD fusion protein binds type I PKA inside cells.

We next expressed the RIAD fusion protein under the mouse *lck* distal promoter (pW120 w/RIAD; Fig. 1*B*) in Jurkat TAg cells. Lysates from transfected cells were subjected to SDS-PAGE and R overlay, demonstrating strong binding of the expressed RIAD fusion protein to radiolabeled RI but not RII (Fig. 1*C*).

Lipid rafts were isolated from pW120 w/RIAD-transfected Jurkat TAg cell lysates by sucrose gradient centrifugation and assessed for levels of RI (Fig. 1*D*, *upper panel*). In cells expressing the RIAD fusion protein, levels of lipid raft associated RI were reduced by 62.5% compared with untransfected cells (Fig. 1*D*, 1*E*). LAT, a lipid raft-associated adaptor protein (36), was used as an internal standard (Fig. 1*D*, *lower panel*, 1*E*). In conclusion, expression of the RIAD fusion protein under the *lck* distal promoter leads to displacement of type I PKA from T cell lipid rafts.

Generation of RIAD-transgenic mice

After verification of the ability of the RIAD fusion protein expressed in T cells under the *lck* distal promoter to displace type I PKA from lipid rafts, we linearized the construct, removed vector-derived sequences, and used the promoter-open reading frame fragment to make RIAD-transgenic mice on a C57BL/6 × CBA background by pronuclear microinjection. Five founder animals were identified using a PCR assay designed to give products of 205 and 335 bp for RIAD-transgenic and wild-type mice, respectively (Fig. 2*A*). Satisfactory expression of the RIAD fusion protein was identified in RIAD-transgenic lines 11 (high expression) and 16 (medium expression) as evident from HA immunoblotting of spleen protein extracts (Fig. 2*B*). The expression pattern of the RIAD fusion protein in RIAD-transgenic line 11 was further investigated by HA immunoblotting of protein extracts from various organs and tissues (Fig. 2*C*, *upper panel*). A GAPDH immunoblot was included as a control for loading and integrity of samples (Fig. 2*C*, *lower panel*). Expression of the RIAD fusion protein was observed in spleen and lymph nodes, as well as in thymus, lung, and small intestine (low levels), which is compatible with the notion of a T cell-specific expression directed by the mouse *lck* distal promoter (25, 37, 38).

$CD3^+$ T cells were negatively selected from a single-cell suspension of mixed spleen cells from RIAD-transgenic and wild-type mice, and expression of the RIAD fusion protein assessed by flow cytometry using fluorochrome-conjugated Ab to CD3 and HA (Fig. 2*D*). Generally, 90–97% of the $CD3^+$ cells expressed the RIAD fusion protein.

Immunofluorescence studies revealed that the RIAD fusion protein (Fig. 2*Eb*, 2*Ee,* 2*Eh*) colocalized with PKA RI (Fig. 2*Ea*, 2*Ec*) and PKA C (Fig. 2*Ed*, 2*Ef*) in splenic T cells from RIAD-transgenic mice. In contrast, PKA RII (Fig. 2*Eg*) localized to the centrosome as earlier reported (19, 39) and did not colocalize with the RIAD fusion protein (Fig. 2*Ei*). Hence the RIAD fusion protein colocalizes with type I PKA in mouse peripheral T cells. Splenic T cell lysates from RIAD-transgenic and wild-type mice

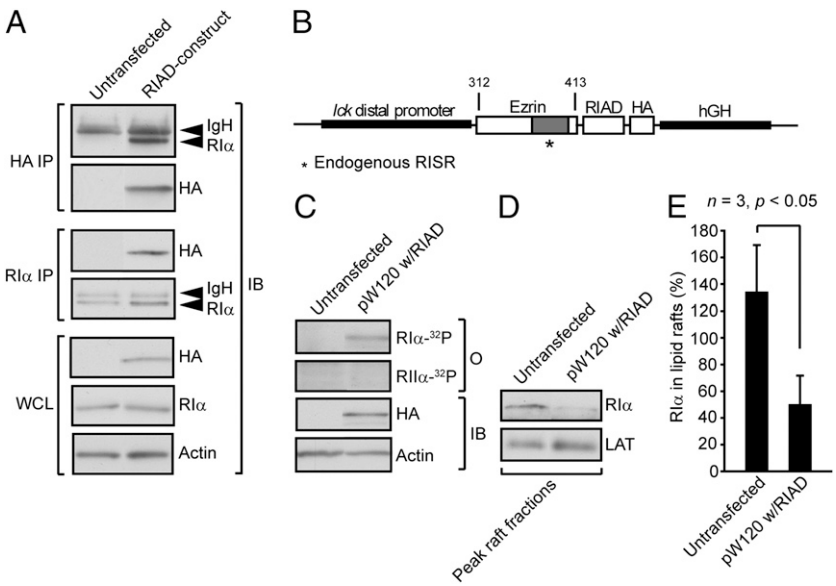

FIGURE 1. RIAD in the context of a soluble ezrin fragment containing the endogenous RISR is expressed in T cells under the *lck* distal promoter and displaces type I PKA from lipid rafts. *A*, COS-7 cells were transfected with 10 μg pFLAG-CMV-5a containing an ezrin fragment encompassing the endogenous RISR coupled to RIAD (see *B*) or left untransfected. The HA-tagged RIAD fusion protein and endogenous RIα were immunoprecipitated from precleared cell lysates (IP). Precipitates were subjected to SDS-PAGE and immunoblotting with the indicated Ab (IB). Expression of the HA-tagged RIAD fusion protein and equal levels of endogenous RIα and actin (loading control) in whole cell lysates (WCL) were confirmed by immunoblotting. *B*, Schematic presentation of the RIAD construct under the mouse *lck* distal promoter in pW120 (pW120 w/RIAD). Amino acid numbers are indicated. hGH, human growth hormone gene. *C*, Jurkat TAg cells were transfected with 80 μg pW120 w/RIAD or left untransfected. Cell lysates were subjected to SDS-PAGE and analyzed for R binding by [^{32}P]-RIα and [^{32}P]-RIIα overlay (O). Expression of the HA-tagged RIAD fusion protein and equal levels of actin (loading control) were confirmed by immunoblotting (IB). *D* and *E*, Jurkat TAg cells were transfected with 40 μg pW120 w/RIAD or left untransfected. The cells were lysed and lipid rafts isolated as described in *Materials and Methods*. Peak raft fractions (fractions 1–5) were pooled and relative levels of RIα in lipid rafts assessed by immunoblotting (*D*) and measured by densitometry (*E*, amalgamated data, mean ± SD). LAT was used as a marker for lipid rafts and as an internal standard. Data presented in *A*, *C*, and *D* are representative of three experiments.

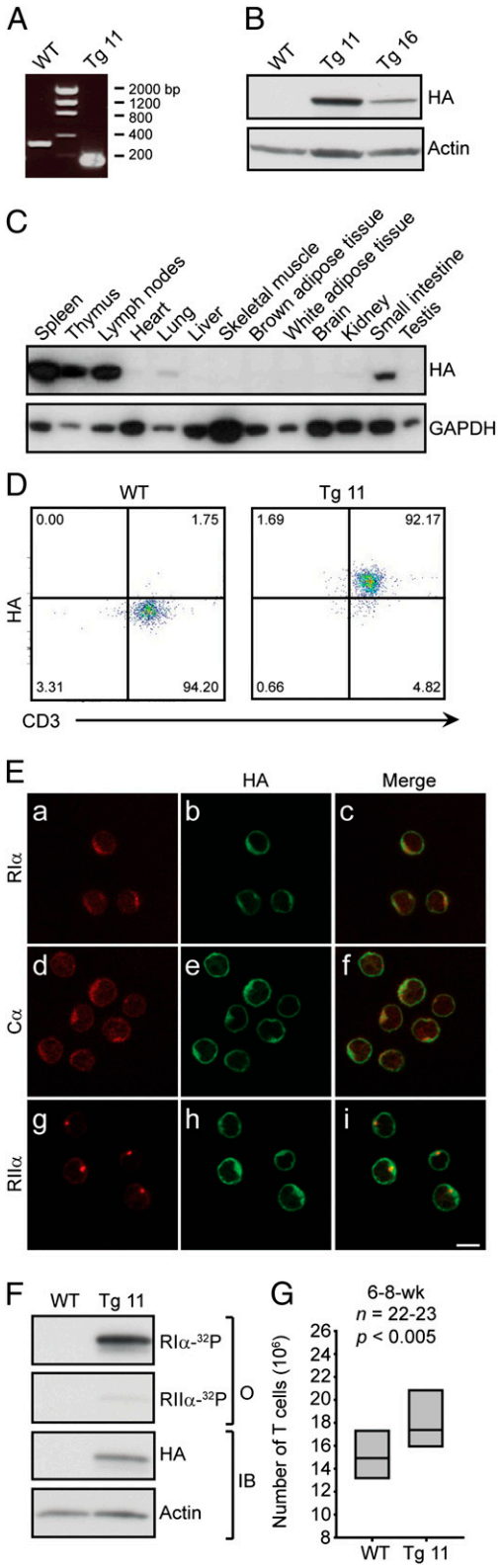

FIGURE 2. Expression of the RIAD fusion protein in mice. *A*, PCR products from analysis of tail biopsies from RIAD-transgenic (Tg 11) and wild-type (WT) mice, separated by agarose gel electrophoresis (205 and 335 bp, respectively, compared with DNA ladder). *B*, Expression of the HA-tagged RIAD fusion protein in spleens from representative RIAD-transgenic mice from high (Tg 11) and medium (Tg 16) expressor lines, assessed by SDS-PAGE (20 μg total protein/lane) and immunoblotting with HA and actin (loading control) Ab. *C*, Tissue (indicated) expression of the HA-tagged RIAD fusion protein in a RIAD-transgenic mouse (Tg 11) assessed by SDS-PAGE (20 μg total protein/lane) and immunoblotting with HA and GAPDH (control for loading and integrity of samples) Ab. *D*, Expression of the HA-tagged RIAD fusion protein in splenic $CD3^+$ T cells from a representative RIAD-transgenic mouse (Tg 11) assessed by intracellular flow cytometry. *E*, Splenic T cells from a RIAD-transgenic mouse (Tg 11) were immunostained for HA (*b*, *e*, *h*), RIα (*a*), Cα (*d*), and RIIα (*g*). Merged images show overlapping subcellular distribution that appears yellow for the HA-tagged RIAD fusion protein and RIα (*c*) and further Cα (*f*), but not for the HA-tagged RIAD fusion protein and RIIα (*i*). Scale bar, 5 μm. *F*, Splenic T cells from a RIAD-transgenic mouse (Tg 11) and a wild-type control (WT) were lysed, subjected to SDS-PAGE, and analyzed for R binding by [^{32}P]-RIα or [^{32}P]-RIIα overlay (O). Expression of the RIAD fusion protein and equal loading (actin) were confirmed by immunoblotting (IB). *G*, T cell counts in spleens from RIAD-transgenic mice (Tg 11) and sex-matched wild-type littermates (WT) of indicated age.

were subjected to SDS-PAGE and R overlays. The RIAD fusion protein bound strongly to radiolabeled RI, but not to RII (Fig. 2*F*). This confirmed that the RIAD fusion protein interacts specifically with type I PKA in T cells also when expressed in vivo in mice.

In general, viable heterozygous RIAD-transgenic mice were born in Mendelian ratios and appeared normal. Spleen T cell counts were, however, significantly higher in 6- to 8-wk-old RIAD-transgenic mice when compared with sex-matched wild-type littermates (Fig. 2*G*). Still, overall spleen weight was not increased in the RIAD-transgenic mice. Furthermore, the percentages of $CD45R\ (B220)^+$ B cells and $CD11b^+$ monocytes/macrophages, as well as the ratio of $CD4^+$ to $CD8^+$ T cells and the percentage of regulatory T cells (Tregs) ($CD4^+CD25^+/CD4^+FOXP3^+$ cells), were not altered in RIAD-transgenic mice compared with sex-matched wild-type littermates (data not shown).

Augmented TCR-proximal signaling in T cells from RIAD-transgenic mice

To assess the level of association of type I PKA with the proximal TCR signaling machinery during T cell activation, we examined localization of CD3 (Fig. 3*Aa*, 3*Ad*) and RI (Fig. 3*Ab*, 3*Ae*) in splenic T cells from RIAD-transgenic and wild-type mice by double-immunofluorescent staining. TCR/CD3 cross-ligation led to activation-dependent capping of CD3 in T cells from both wild-type and transgenic mice (Fig. 3*Aa*, 3*Ad*). Whereas RI colocalized with the CD3 cap in T cells from wild-type mice (Fig. 3*Ac*) consistent with earlier observations (4), RI colocalization with CD3 was reduced by 38% in T cells from RIAD-transgenic mice (Fig. 3*Af*, 3*B*). Thus, the inhibitory cAMP–type I PKA pathway appears to be partially disrupted in peripheral T cells from RIAD-transgenic mice.

We next examined the effect of RI anchoring disruption on proximal TCR signaling. Although activation by CD3 cross-ligation is sufficient to trigger TCR-proximal signaling in human T cells (40), CD4 costimulation is needed in mouse T cells (R. Mosenden, I. Cornez, K. Tasken, unpublished observations and Ref. 41). Splenic T cells from 6- to 8-wk-old RIAD-transgenic mice and sex-matched wild-type littermates were stimulated by CD3/CD4 cross-ligation and kinetics of phosphorylation of individual proteins in the TCR signaling cascade assessed by immunoblotting for phosphotyrosine, pSrc family (Y416) to detect phosphorylated lymphocyte-specific protein-tyrosine kinase (pLck; Y394) and pAkt (T308). The pSrc family (Y416) Ab detects all Src family protein tyrosine kinases phosphorylated on the conserved activating tyrosine residue, for example, Y416 in Src and Y394 in Lck. Expression of the RIAD fusion protein and equal loading were confirmed by HA epitope and actin immunoblotting, respectively (Fig. 3*C*). Amalgamated data from several experiments demonstrated that the basal level of phosphorylation of

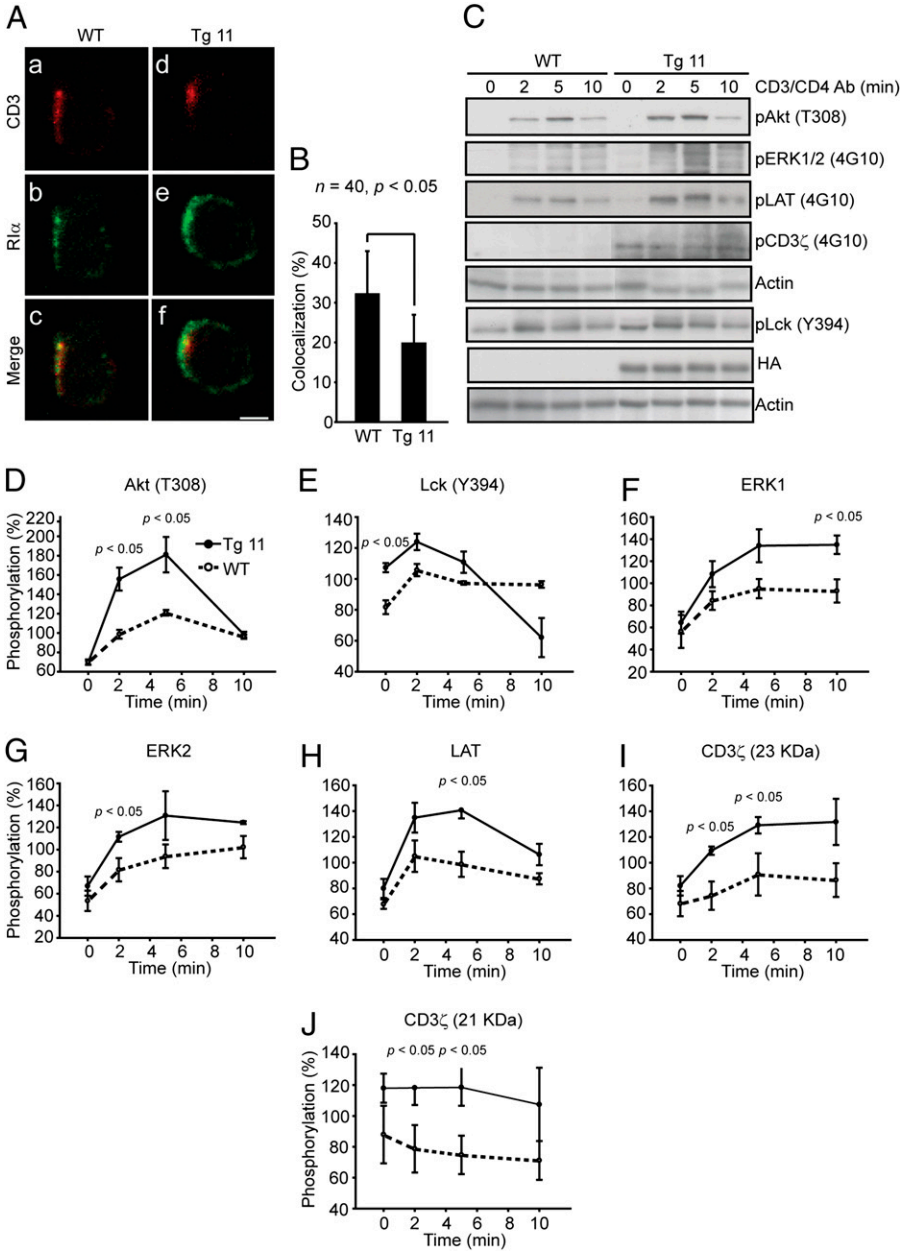

FIGURE 3. Displacement of type I PKA from the TCR-proximal signaling machinery results in enhanced downstream signaling in peripheral T cells from RIAD-transgenic mice. *A*, Localization of TCR/CD3 (*a*, *d*) and RIα (*b*, *e*) in splenic T cells from RIAD-transgenic (Tg 11, *d–f*) and wild-type (WT, *a–c*) mice after capping of the TCR/CD3 using biotin-conjugated CD3 Ab and subsequently fluorochrome-conjugated streptavidin as assessed by immunofluorescence analysis. Merged images show overlapping subcellular distribution that appears yellow (*c*, *f*). Scale bar, 2 μm. *B*, Analysis of colocalization of TCR/CD3 and RIα in activated RIAD-transgenic (Tg 11) and wild-type (WT) splenic T cells. Colocalization ratios were calculated from double-positive pixels divided by all stained pixels (mean ± SD). *C*, Splenic T cells from 6-to 8-wk-old RIAD-transgenic mice (Tg 11) and sex-matched wild-type littermates (WT) were activated for the indicated periods by CD3/CD4 Ab cross-ligation. The phosphorylation status of the indicated proteins, expression of the RIAD fusion protein, and equal loading (actin) were assessed by SDS-PAGE and immunoblotting. Data presented are representative of three experiments. *D–J*, Relative levels of phosphorylation from experiments as in *C* measured by densitometry (n = 3, mean ± SEM). Actin was used as an internal standard.

Lck was significantly enhanced in RIAD-transgenic mouse T cells (Fig. 3*E*). Furthermore, postactivation, CD3ζ, LAT, ERK, and Akt were more extensively phosphorylated in T cells from RIAD-transgenic mice (Fig. 3*D*, 3*F–J*). Together, this indicates that uncoupling of the cAMP negative feedback loop results in enhanced TCR signaling in peripheral T cells from RIAD-transgenic mice.

Enhanced T cell responses in RIAD-transgenic mice

From studies of T cell signaling, we proceeded to examine functional responses of T cells from RIAD-transgenic mice. Splenic T cells from RIAD-transgenic mice and sex-matched wild-type littermates were activated by CD3/CD28 cross-ligation for 20 h and cytokine secretion levels determined. T cells from RIAD-transgenic mice displayed enhanced immune responsiveness assessed as IL-2 secretion compared with T cells from wild-type littermates (Fig. 4*A*). TNF-α production (Fig. 4*H*) was also increased in T cells from RIAD-transgenic mice compared with T cells from wild-type littermates. In comparison, secretion of IL-4, IL-5, IL-10, IL-12, GM-CSF, and IFN-γ (Fig. 4*B–G*) did not significantly differ between T cells from RIAD-transgenic mice and T cells from wild-type littermates. Thus, T cell-specific perturbation of the inhibitory cAMP–type I PKA pathway results in hyperresponsive T cells and increased secretion of the proinflammatory cytokine TNF-α in RIAD-transgenic mice, which indicates that this pathway imposes a tonic level of inhibition on T cell immune responses.

Altered PGE_2 and cAMP sensitivity in T cells from RIAD-transgenic mice

To determine the effect of RI anchoring disruption on T cell immune function in a situation where extracellular stimuli turn on the inhibitory cAMP–type I PKA pathway, we preincubated splenic T cells from 6- to 8-wk-old RIAD-transgenic mice and sex-matched wild-type littermates with increasing concentrations of a cell-permeable analog of cAMP, 8-CPT-cAMP, and proceeded to activate the cells and assess T cell immune responsiveness, measured as IL-2 secretion. This experiment demonstrated that 8-

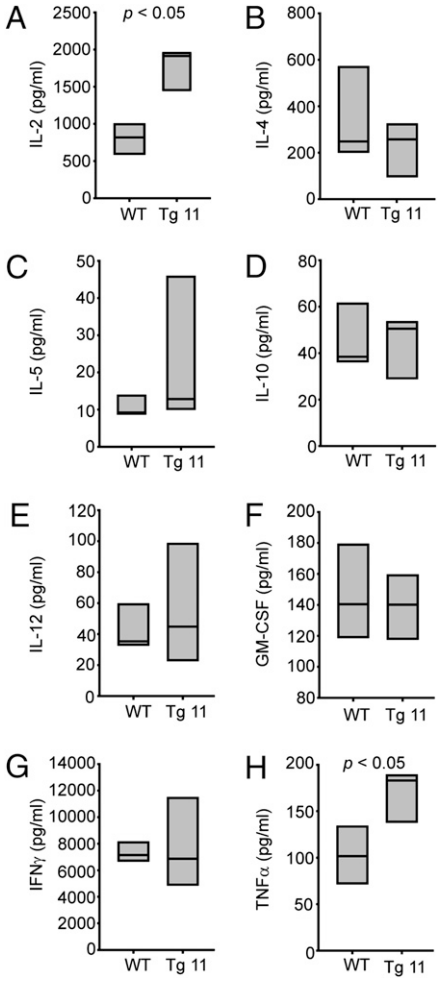

FIGURE 4. Enhanced T cell responses in RIAD-transgenic mice. Splenic T cells from 4- to 5-mo-old RIAD-transgenic mice (Tg 11) and sex-matched wild-type littermates (WT), n = 3–4, were stimulated by CD3/CD28 cross-ligation for 20 h and secretion of cytokines measured by ELISA (*A*) or multiplex assay (*B–H*).

CPT-cAMP inhibited IL-2 secretion in a concentration-dependent fashion with an IC_{50} of 0.4 μM for wild-type T cells. For RIAD-transgenic T cells, the inhibition curve was right shifted, with an apparent IC_{50} of 1.4 μM (Fig. 5*A*). When 20 pairs of 6- to 8-wk-old wild-type controls (sex-matched littermates) and RIAD-transgenic mice were compared, the average IC_{50} (8-CPT-cAMP) values for cAMP-mediated inhibition of IL-2 secretion were 0.6 and 1.0 μM, respectively (Fig. 5*B*). Next, splenic T cells from a 4- to 5-mo-old RIAD-transgenic mouse and a sex-matched wild-type littermate were preincubated with increasing concentrations of PGE_2 and subsequently activated via the TCR. PGE_2 inhibited IL-2 secretion in a dose-dependent manner with an IC_{50} of 1.5 nM for wild-type T cells. For RIAD-transgenic T cells, the inhibition curve was right shifted with an IC_{50} of 29.9 nM (Fig. 5*C*). We conclude that peripheral T cells from RIAD-transgenic mice display a reduced sensitivity to cAMP-mediated inhibition of T cell function.

Resistance to disease progression in LP-BM5–infected RIAD-transgenic mice

Because hyperactivation of the cAMP–type I PKA pathway is involved in the T cell dysfunction in MAIDS (16, 17), as well as HIV infection (18), we wanted to investigate the consequences of T cell-specific type I PKA anchoring disruption on MAIDS disease progression. Six- to 8-wk-old RIAD-transgenic mice and sex-matched wild-type littermates were injected four times (i.p.) at 1-wk intervals with LP-BM5 extract. Eight to 9 wk after the last injection, MAIDS-associated splenomegaly and lymphadenopathy were apparent in the wild-type mice (Fig. 6*A*, *middle panel*), but clearly less manifest in the RIAD-transgenic mice (Fig. 6*A*, *right panel*). In PBS-injected C57BL/6 control mice, spleen and lymph node sizes were normal (Fig. 6*A*, *left panel*). Spleen (Fig. 6*B*) and lymph node (Fig. 6*C*) weights were significantly lower in LP-BM5–infected RIAD-transgenic mice compared with LP-BM5–infected sex-matched wild-type littermates. Thus, MAIDS-associated spleen and lymph node enlargement is limited in RIAD-transgenic mice.

The ability of T cells to proliferate in response to CD3 stimulation declines progressively during the course of MAIDS, partially because of high intracellular levels of cAMP and the resulting type I PKA-mediated inhibition of T cell activation (16, 17). In this study, lymph node cells from LP-BM5–infected RIAD-transgenic mice and sex-matched wild-type littermates were stimulated with soluble CD3 Ab and/or IL-2 for 72 h and proliferation assessed as [^{3}H]thymidine incorporation. Proliferation in response to soluble CD3 Ab alone, IL-2 alone, and soluble CD3 Ab and IL-2 in combination was significantly higher in the RIAD-transgenic mice compared with sex-matched wild-type littermates. In fact, lymph node cell proliferation in LP-BM5–infected RIAD-transgenic mice was almost the same as in uninfected C57BL/6 control mice on stimulation with soluble CD3 Ab alone or in combination with IL-2 (Fig. 6*D*). Thus, MAIDS-associated T cell anergy is broken and T cell proliferative function maintained in RIAD-transgenic mice.

Finally, LP-BM5 viral load in infected RIAD-transgenic mice and sex-matched wild-type littermates was assessed as abundance of BM5def mRNA relative to B2M mRNA by reverse transcription and quantitative real-time PCR (Fig. 6*E*). Viral load was significantly lower in LP-BM5–infected RIAD-transgenic mice compared with LP-BM5–infected sex-matched wild-type littermates, indicating improved ability to compete virus replication in the RIAD-transgenic mice.

Development of MAIDS phenotypic characteristics is inhibited in infected RIAD-transgenic mice

A large proportion of $CD4^+$ T cells is characterized by an unusual CD90.2 (Thy-1.2)-negative phenotype in LP-BM5–infected mice compared with uninfected controls (42, 43) (Fig. 7*A*, *middle* and *left panels*). We have previously shown that the loss of CD90.2 correlates with increased intracellular cAMP concentration and activation of type I PKA (16). To examine the $CD4^+CD90.2^-$ T cell population in LP-BM5–infected RIAD-transgenic mice, lymph node cells from LP-BM5–infected RIAD-transgenic mice and sex-matched wild-type littermates, as well as uninfected C57BL/6 control mice, were stained with fluorochrome-conjugated Ab to surface Ags and analyzed by flow cytometry. This revealed a significantly smaller $CD4^+CD90.2^-$ T cell population in LP-BM5–infected RIAD-transgenic mice compared with in LP-BM5–infected wild-type littermates (Fig. 7*A*, *right* and *middle panels*, 7*B*). Furthermore, MAIDS is associated with an expansion of B cells expressing CD45R (B220) at low densities (CD45R dim cells) (44) (Fig. 7*C*, *middle* and *left panels*). This expansion was limited in LP-BM5–infected RIAD-transgenic mice (Fig. 7*C*, *right panel*, 7*D*). CD11b, normally expressed on resting monocytes and macrophages, is also upregulated on LP-BM5–infected T and B cells (17) (Fig. 7*E*, *middle* and *left panels*). In LP-BM5–infected RIAD-transgenic mice, however, the expression of CD11b on B cells is limited (Fig. 7*E*, *right panel*, 7*F*). Finally, the expression

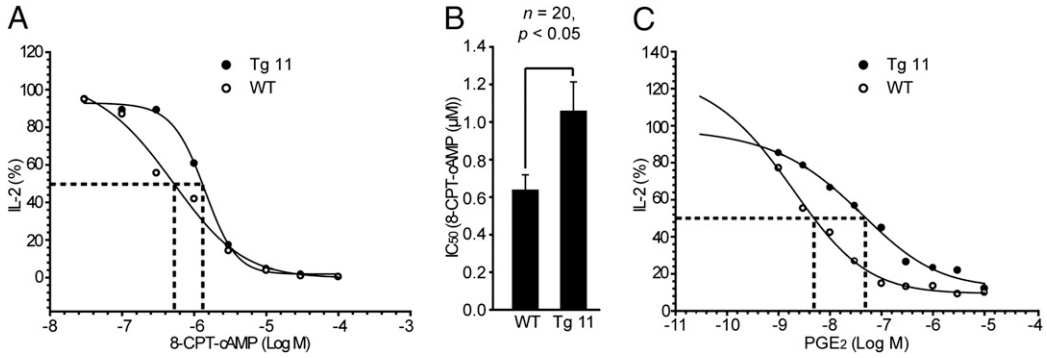

FIGURE 5. Reduced sensitivity to cAMP-mediated inhibition of TCR-induced IL-2 secretion in peripheral T cells from RIAD-transgenic mice. *A* and *B*, Splenic T cells from 6- to 8-wk-old RIAD-transgenic mice (Tg 11) and sex-matched wild-type littermates (WT) were incubated with increasing concentrations of 8-CPT-cAMP, stimulated by CD3/CD28 cross-ligation for 20 h, and subsequently analyzed for IL-2 secretion by ELISA. IC_{50} values were estimated by nonlinear regression analyses in SigmaPlot (SPSS) as indicated. *A*, Representative experiment from one Tg 11/WT pair. *B*, Amalgamated data from cAMP sensitivity analyses expressed as IC_{50} (8-CPT-cAMP) values (mean ± SEM). *C*, Splenic T cells from a 4- to 5-mo-old RIAD-transgenic mouse (Tg 11) and a sex-matched wild-type littermate (WT) were incubated with increasing concentrations of PGE_2, stimulated by CD3/CD28 cross-ligation for 20 h, and analyzed for IL-2 secretion by ELISA. IC_{50} values were estimated by nonlinear regression analyses in SigmaPlot (SPSS) as indicated.

of programmed death 1 (PD-1) on T cells is upregulated in LP-BM5–infected wild-type mice (Fig. 7*G*, *middle* and *left panels*), but the upregulation on T cells from LP-BM5–infected RIAD-transgenic mice is limited (Fig. 7*G*, *right panel*, 7*H*). We conclude that the emergence of cell populations characteristic for MAIDS is limited in infected RIAD-transgenic mice.

Discussion

In 2002, Williams (45) showed that incubation of mouse spleen cells with the PKA anchoring disruptor peptide Ht31 leads to increased IL-2, IL-4, IL-5, and IFN-γ secretion, as well as enhanced Ag-induced proliferation, suggesting that anchored PKA activity was necessary for maintaining T cells in a resting state. Ht31-treated mouse spleen cells were insensitive to the inhibitory effect of cAMP on IL-2 production, indicating that anchored PKA activity was necessary for cAMP-mediated inhibition of T cell function. cAMP modulates T cell immune function at multiple levels through PKA (46). However, the importance of cAMP-type I PKA-mediated inhibition of T cell activation has been demonstrated by RIAD-mediated displacement of type I PKA from lipid rafts, resulting in reduced phosphorylation of Lck Y505 (19). Furthermore, knockdown of ezrin using RNA interference (9), expression of mutant ezrin forms where type I PKA binding has been abrogated by substitutions in the endogenous RISR sequence (20) and loading of cells with a peptide that competes the ezrin–EBP50 interaction (12) reversed cAMP-mediated suppression of IL-2 production in primary human T cells. Likewise, proteolytically stable RIAD peptidomimetics (47) and the RISR peptide (20) prevented cAMP-mediated inhibition of primary human T cell function. Finally, specific activation of type I PKA was shown to be necessary and sufficient for mediating the inhibitory effect of cAMP on proliferation of primary human T cells (3).

As stated, type I PKA is targeted to lipid rafts and the signaling machinery immediately downstream of the TCR by ezrin (9). Ezrin is a dual-specificity AKAP that contains two R binding regions: the AKB, which is present in almost all AKAPs, and the upstream RISR, which is present in dual-specificity AKAPs and serves to enhance and specify binding to type I PKA. We have previously shown by R overlay and amplified luminescence ligand proximity assay (AlphaScreen) that when combined with RIAD, the RISR enhances binding to RIα, and that a mutation in the ezrin endogenous RISR (R381A) diminishes colocalization with RIα and restores cAMP-mediated inhibition of IL-2 production in primary human T cells (20). In this study, we engineered a construct directing the expression of a soluble ezrin fragment with the endogenous RISR and RIAD inserted in the position of the endogenous AKB in mouse peripheral T cells. This RIAD fusion protein retained RI selectivity and the capability to compete type I PKA anchoring to lipid rafts and the proximal TCR signaling machinery.

The RIAD-transgenic mice had increased peripheral T cell counts. This may be partly explained by augmented activation of Akt, which mediates T cell survival (48), in activated RIAD-transgenic T cells. Furthermore, perturbation of the inhibitory cAMP–type I PKA pathway leads to enhanced TCR-proximal signaling and increased IL-2 secretion from activated T cells. IL-2 promotes proliferation of T cells (49). However, despite the increased T cell counts, spleens of RIAD-transgenic mice were not enlarged. In addition, the percentage of B cells and monocytes/macrophages were the same in RIAD-transgenic mice and sex-matched wild-type littermates, as were the ratio of $CD4^+$ to $CD8^+$ T cells and the fraction of Treg, but fewer other leukocytes, erythrocytes, platelets, or parenchymal cells may allow for increased T cell counts but unaltered spleen size.

Cyclic AMP-elevating or -mimicking agents inhibit production of the Th1 cytokines IL-12, IFN-γ, and IL-2, as well as TNF-α, whereas production of the Th2 cytokines IL-4, IL-5, IL-6, and IL-10 remains unchanged or even enhanced (18, 50–53). In line with this, we did observe significantly increased secretion of IL-2 and TNF-α, and in addition, a possible increased secretion of IL-12 and IFN-γ, from activated RIAD-transgenic T cells. In contrast, secretion of the Th2 cytokines IL-4 and IL-10 was unaffected or possibly reduced. Williams (45) showed that incubation of mouse spleen cells with the unspecific PKA anchoring disruptor Ht31 resulted in increased secretion of IFN-γ, IL-2, IL-4, and IL-5 from activated T cells. The discrepancies between our results and those of Williams (45) may be because of the different cell populations used and the fact that Ht31 disrupts anchoring of both type I and II PKA, whereas the RIAD fusion protein specifically disrupts type I PKA anchoring.

We demonstrate that peripheral T cells from RIAD-transgenic mice are less sensitive to PGE_2- and cAMP-mediated inhibition of T cell function, and thus display a reduced threshold for activation. The RIAD-transgenic T cells are hyperreactive and hyperresponsive. Induction of cAMP levels in responder T cells, either via secretion of PGE_2 (54) or adenosine (55, 56) or via

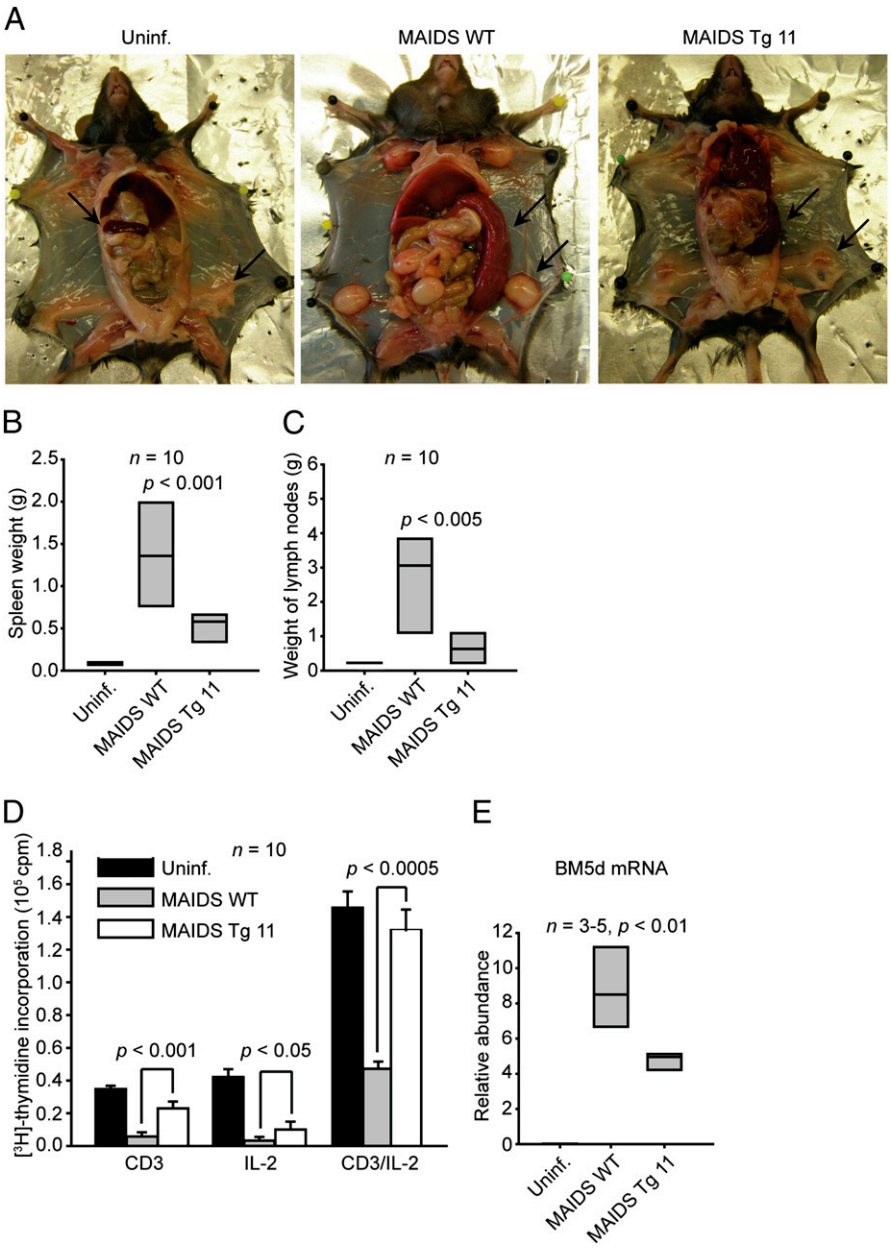

FIGURE 6. Lower viral load and inhibited development of MAIDS-associated splenomegaly, lymphadenopathy, and T cell anergy in RIAD-transgenic mice. Six- to 8-wk-old RIAD-transgenic mice and sex-matched wild-type littermates were injected four times i.p., at 1-wk interval, with LP-BM5 (MAIDS Tg 11 and MAIDS WT, respectively). Age- and sex-matched C57BL/6 control mice were correspondingly injected with PBS (Uninf.). The mice were sacrificed 8–9 wks after the last injection (*A*, representative animals). Spleens (*B*) and lymph nodes (*C*) (indicated by arrows in *A*) were dissected and weighed. *D*, Lymph node cells from LP-BM5–infected RIAD-transgenic mice (MAIDS Tg 11) and sex-matched wild-type littermates (MAIDS WT), as well as age- and sex-matched uninfected C57BL/6 control mice (Uninf.), were stimulated with soluble CD3 Ab and/or IL-2 for 72 h and proliferation assessed as [^{3}H]thymidine incorporation during the last 4 h (mean ± SEM). *E*, RNA was extracted from LP-BM5–infected RIAD-transgenic mice (MAIDS Tg 11) and sex-matched wild-type littermates (MAIDS WT) and age- and sex-matched uninfected C57BL/6 control mice (Uninf.), reversely transcribed, and abundance of BM5def mRNA relative to B2M mRNA was assessed by quantitative real-time PCR.

direct intercellular transfer of cAMP by means of gap junctions (57), has recently been appreciated as one of the mechanisms by which Treg execute their suppressive action. It is therefore tempting to speculate that RIAD-transgenic responder T cells may be resistant to Treg-mediated suppression. Further investigation will reveal whether this is indeed the case and also whether RIAD-transgenic mice, with partly cAMP-resistant effector T cells, are less prone to tumor development because of lack of local inhibition of antitumor immune activity by Treg. Furthermore, hyperreactive T cells and possible resistance to Treg-mediated immune modulation could potentially lead to autoimmune disease in the RIAD-transgenic mice. However, no signs of spontaneous autoimmunity were seen in RIAD-transgenic mice maintained up to ~2 y of age. Further investigation will be needed to elucidate whether RIAD-transgenic mice display increased susceptibility to induced autoimmune diseases.

Hyperactivation of the cAMP–type I PKA pathway has been implicated in the T cell dysfunction associated with HIV infection (18) and a subset of common variable immunodeficiency (58), and is also involved in the T cell dysfunction in MAIDS (16, 17). Blocking this pathway by means of the type I PKA-specific antagonist Rp-8-Br-cAMPS or cyclooxygenase inhibitors limiting the production of PGE_2 restores T cell function in vitro in MAIDS (16, 17) and in HIV infection (18). In this article, we show that T cell-specific type I PKA anchoring disruption limits the splenomegaly and lymphadenopathy associated with MAIDS. Furthermore, the MAIDS-associated abundance of $CD4^+CD90.2^-$ T cells, CD45R dim B cells, $CD45R^+CD11b^+$ B cells, and $CD3^+$ $PD\text{-}1^+$ T cells is limited, T cell proliferative responses maintained, and viral replication better controlled in the RIAD-transgenic mice. The latter finding is particularly interesting and does suggest that maintained T cell function indeed contributes to improved viral control in MAIDS, a thought also supported by a report showing that CTL play a crucial role in the resistance of some mice strains to LP-BM5 infection (59). Some steps in the viral cycle may depend on PKA activity. This is indeed the case in HIV infection, where activation of the cAMP–PKA pathway has been shown to increase virus transcription (60). In HIV infection, undefined events involved in viral entry and infectivity are also under control of PKA (61, 62). Finally, PKA-mediated phos-

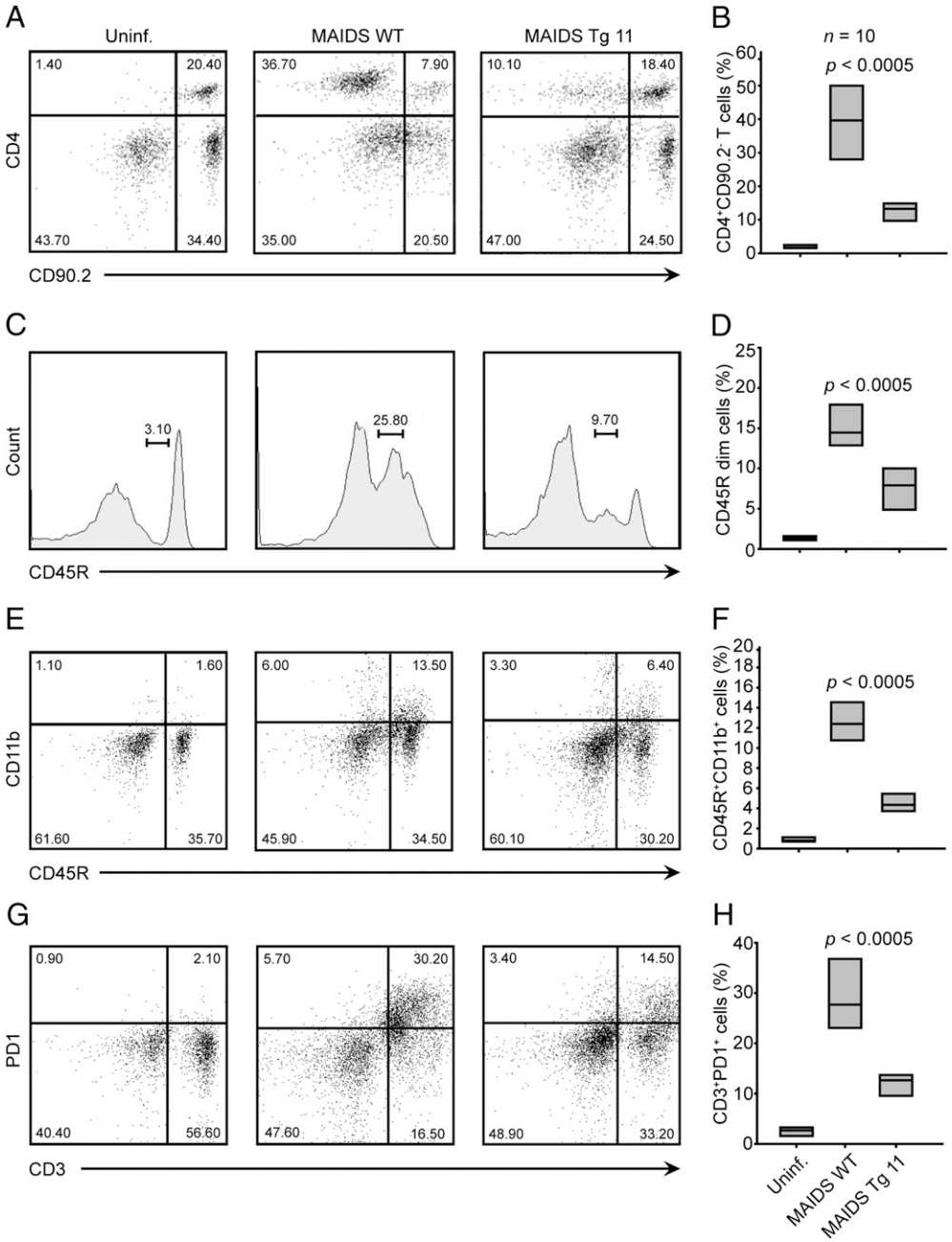

FIGURE 7. Inhibited MAIDS phenotypic changes in infected RIAD-transgenic mice. Lymph node cells from LP-BM5–infected RIAD-transgenic mice (MAIDS Tg 11) and sex-matched wild-type littermates (MAIDS WT), as well as age- and sex-matched uninfected C57BL/6 control mice (Uninf.), were stained with fluorochrome-conjugated Ab, and the percentages of $CD4^+CD90.2^-$ T cells (*A*, *B*), CD45R dim cells (*C*, *D*), $CD45R^+CD11b^+$ cells (*E*, *F*), and $CD3^+PD\text{-}1^+$ cells (*G*, *H*) were determined by flow cytometry. *A*, *C*, *E*, and *G*, Cells from representative animals.

phorylation of the HIV-1 accessory proteins Nef and viral protein R is necessary for HIV-1 pathology (63, 64). An approach targeting the cAMP–type I PKA pathway could, therefore, have several advantages in HIV infection, preserving innate and adaptative immune responses on the one hand, and directly limiting infectivity on the other hand. Thus, our findings underscore the inhibitory cAMP–type I PKA pathway in T cells as a putative target for therapeutic intervention in T cell immunodeficiencies.

Acknowledgments

We thank Gladys M. Tjørhom, Jorun Solheim, Guri Opsahl, and Dr. Eshrat Babaie for excellent technical assistance; Dr. Sandra Ormenese and the GIGA-R imaging core facility at University of Liège, Laboratory of Immunology and Infectious Diseases, Liège-Sart Tilman, Belgium, for help with flow cytometry; the National Lab Animal Center at the Norwegian Institute of Public Health, Oslo, Norway, and the GIGA-R animal facility for assistance with mice handling. We also thank Drs. Line M. G. Wang, Oliwia Witczak, Cathrine R. Carlson, Knut M. Torgersen, Michael Leitges, and Ludvig A. Munthe for discussions and advice.

Disclosures

The authors have no financial conflicts of interest.

References

1. Vang, T., K. M. Torgersen, V. Sundvold, M. Saxena, F. O. Levy, B. S. Skålhegg, V. Hansson, T. Mustelin, and K. Taskén. 2001. Activation of the COOH-terminal Src kinase (Csk) by cAMP-dependent protein kinase inhibits signaling through the T cell receptor. *J. Exp. Med.* 193: 497–507.

2. Schillace, R. V., S. F. Andrews, S. G. Galligan, K. A. Burton, H. J. Starks, H. G. Bouwer, G. S. McKnight, M. P. Davey, and D. W. Carr. 2005. The role of protein kinase A anchoring via the RII alpha regulatory subunit in the murine immune system. *J. Immunol.* 174: 6847–6853.
3. Skålhegg, B. S., B. F. Landmark, S. O. Døskeland, V. Hansson, T. Lea, and T. Jahnsen. 1992. Cyclic AMP-dependent protein kinase type I mediates the inhibitory effects of 3′,5′-cyclic adenosine monophosphate on cell replication in human T lymphocytes. *J. Biol. Chem.* 267: 15707–15714.
4. Skålhegg, B. S., K. Taskén, V. Hansson, H. S. Huitfeldt, T. Jahnsen, and T. Lea. 1994. Location of cAMP-dependent protein kinase type I with the TCR-CD3 complex. *Science* 263: 84–87.
5. Brdicka, T., D. Pavlistová, A. Leo, E. Bruyns, V. Korínek, P. Angelisová, J. Scherer, A. Shevchenko, I. Hilgert, J. Cerný, et al. 2000. Phosphoprotein associated with glycosphingolipid-enriched microdomains (PAG), a novel ubiquitously expressed transmembrane adaptor protein, binds the protein tyrosine kinase csk and is involved in regulation of T cell activation. *J. Exp. Med.* 191: 1591–1604.
6. Kawabuchi, M., Y. Satomi, T. Takao, Y. Shimonishi, S. Nada, K. Nagai, A. Tarakhovsky, and M. Okada. 2000. Transmembrane phosphoprotein Cbp regulates the activities of Src-family tyrosine kinases. *Nature* 404: 999–1003.
7. Chow, L. M., M. Fournel, D. Davidson, and A. Veillette. 1993. Negative regulation of T-cell receptor signalling by tyrosine protein kinase p50csk. *Nature* 365: 156–160.
8. Okada, M., S. Nada, Y. Yamanashi, T. Yamamoto, and H. Nakagawa. 1991. CSK: a protein-tyrosine kinase involved in regulation of src family kinases. *J. Biol. Chem.* 266: 24249–24252.
9. Ruppelt, A., R. Mosenden, M. Grönholm, E. M. Aandahl, D. Tobin, C. R. Carlson, H. Abrahamsen, F. W. Herberg, O. Carpén, and K. Taskén. 2007. Inhibition of T cell activation by cyclic adenosine 5′-monophosphate requires lipid raft targeting of protein kinase A type I by the A-kinase anchoring protein ezrin. *J. Immunol.* 179: 5159–5168.
10. Brdicková, N., T. Brdicka, L. Andera, J. Spicka, P. Angelisová, S. L. Milgram, and V. Horejsí. 2001. Interaction between two adapter proteins, PAG and EBP50: a possible link between membrane rafts and actin cytoskeleton. *FEBS Lett.* 507: 133–136.
11. Itoh, K., M. Sakakibara, S. Yamasaki, A. Takeuchi, H. Arase, M. Miyazaki, N. Nakajima, M. Okada, and T. Saito. 2002. Cutting edge: negative regulation of immune synapse formation by anchoring lipid raft to cytoskeleton through Cbp-EBP50-ERM assembly. *J. Immunol.* 168: 541–544.
12. Stokka, A. J., R. Mosenden, A. Ruppelt, B. Lygren, and K. Taskén. 2010. The adaptor protein EBP50 is important for localization of the protein kinase A-Ezrin complex in T-cells and the immunomodulating effect of cAMP. *Biochem. J.* 425: 381–388.
13. Algrain, M., O. Turunen, A. Vaheri, D. Louvard, and M. Arpin. 1993. Ezrin contains cytoskeleton and membrane binding domains accounting for its proposed role as a membrane-cytoskeletal linker. *J. Cell Biol.* 120: 129–139.
14. Aziz, D. C., Z. Hanna, and P. Jolicoeur. 1989. Severe immunodeficiency disease induced by a defective murine leukaemia virus. *Nature* 338: 505–508.
15. Chattopadhyay, S. K., D. N. Sengupta, T. N. Fredrickson, H. C. Morse, III, and J. W. Hartley. 1991. Characteristics and contributions of defective, ecotropic, and mink cell focus-inducing viruses involved in a retrovirus-induced immunodeficiency syndrome of mice. *J. Virol.* 65: 4232–4241.
16. Rahmouni, S., E. M. Aandahl, M. Trebak, J. Boniver, K. Taskén, and M. Moutschen. 2001. Increased cAMP levels and protein kinase (PKA) type I activation in CD4+ T cells and B cells contribute to retrovirus-induced immunodeficiency of mice (MAIDS): a useful in vivo model for drug testing. *FASEB J.* 15: 1466–1468.
17. Rahmouni, S., E. M. Aandahl, B. Nayjib, M. Zeddou, S. Giannini, M. Verlaet, R. Greimers, J. Boniver, K. Taskén, and M. Moutschen. 2004. Cyclo-oxygenase type 2-dependent prostaglandin E2 secretion is involved in retrovirus-induced T-cell dysfunction in mice. *Biochem. J.* 384: 469–476.
18. Aandahl, E. M., P. Aukrust, B. S. Skålhegg, F. Müller, S. S. Frøland, V. Hansson, and K. Taskén. 1998. Protein kinase A type I antagonist restores immune responses of T cells from HIV-infected patients. *FASEB J.* 12: 855–862.
19. Carlson, C. R., B. Lygren, T. Berge, N. Hoshi, W. Wong, K. Taskén, and J. D. Scott. 2006. Delineation of type I protein kinase A-selective signaling events using an RI anchoring disruptor. *J. Biol. Chem.* 281: 21535–21545.
20. Jarnaess, E., A. Ruppelt, A. J. Stokka, B. Lygren, J. D. Scott, and K. Taskén. 2008. Dual specificity A-kinase anchoring proteins (AKAPs) contain an additional binding region that enhances targeting of protein kinase A type I. *J. Biol. Chem.* 283: 33708–33718.
21. Kozak, M. 1986. Point mutations define a sequence flanking the AUG initiator codon that modulates translation by eukaryotic ribosomes. *Cell* 44: 283–292.
22. Brinster, R. L., J. M. Allen, R. R. Behringer, R. E. Gelinas, and R. D. Palmiter. 1988. Introns increase transcriptional efficiency in transgenic mice. *Proc. Natl. Acad. Sci. USA* 85: 836–840.
23. Palmiter, R. D., E. P. Sandgren, M. R. Avarbock, D. D. Allen, and R. L. Brinster. 1991. Heterologous introns can enhance expression of transgenes in mice. *Proc. Natl. Acad. Sci. USA* 88: 478–482.
24. Wildin, R. S., A. M. Garvin, S. Pawar, D. B. Lewis, K. M. Abraham, K. A. Forbush, S. F. Ziegler, J. M. Allen, and R. M. Perlmutter. 1991. Developmental regulation of lck gene expression in T lymphocytes. *J. Exp. Med.* 173: 383–393.
25. Wildin, R. S., H. U. Wang, K. A. Forbush, and R. M. Perlmutter. 1995. Functional dissection of the murine lck distal promoter. *J. Immunol.* 155: 1286–1295.
26. Brinster, R. L., H. Y. Chen, M. E. Trumbauer, M. K. Yagle, and R. D. Palmiter. 1985. Factors affecting the efficiency of introducing foreign DNA into mice by microinjecting eggs. *Proc. Natl. Acad. Sci. USA* 82: 4438–4442.
27. Gordon, J. W., G. A. Scangos, D. J. Plotkin, J. A. Barbosa, and F. H. Ruddle. 1980. Genetic transformation of mouse embryos by microinjection of purified DNA. *Proc. Natl. Acad. Sci. USA* 77: 7380–7384.
28. Jaenisch, R. 1988. Transgenic animals. *Science* 240: 1468–1474.
29. Clipstone, N. A., and G. R. Crabtree. 1992. Identification of calcineurin as a key signalling enzyme in T-lymphocyte activation. *Nature* 357: 695–697.
30. Taskén, K., K. B. Andersson, B. S. Skålhegg, K. A. Taskén, V. Hansson, T. Jahnsen, and H. K. Blomhoff. 1993. Reciprocal regulation of mRNA and protein for subunits of cAMP-dependent protein kinase (RI alpha and C alpha) by cAMP in a neoplastic B cell line (Reh). *J. Biol. Chem.* 268: 23483–23489.
31. Carr, D. W., R. E. Stofko-Hahn, I. D. Fraser, S. M. Bishop, T. S. Acott, R. G. Brennan, and J. D. Scott. 1991. Interaction of the regulatory subunit (RII) of cAMP-dependent protein kinase with RII-anchoring proteins occurs through an amphipathic helix binding motif. *J. Biol. Chem.* 266: 14188–14192.
32. Durgerian, S., and S. S. Taylor. 1989. The consequences of introducing an autophosphorylation site into the type I regulatory subunit of cAMP-dependent protein kinase. *J. Biol. Chem.* 264: 9807–9813.
33. Hausken, Z. E., V. M. Coghlan, and J. D. Scott. 1998. Overlay, ligand blotting, and band-shift techniques to study kinase anchoring. *Methods Mol. Biol.* 88: 47–64.
34. Lygren, B., K. Taskén, and C. R. Carlson. 2005. A fast and sensitive method for isolation of detergent-resistant membranes from T cells. *J. Immunol. Methods* 305: 199–205.
35. Haas, M., and T. Reshef. 1980. Non-thymic malignant lymphomas induced in C57BL/6 mice by cloned dualtropic viruses isolated from hematopoietic stromal cell lines. *Eur. J. Cancer* 16: 909–917.
36. Zhang, W., R. P. Trible, and L. E. Samelson. 1998. LAT palmitoylation: its essential role in membrane microdomain targeting and tyrosine phosphorylation during T cell activation. *Immunity* 9: 239–246.
37. Perlmutter, R. M., J. D. Marth, D. B. Lewis, R. Peet, S. F. Ziegler, and C. B. Wilson. 1988. Structure and expression of lck transcripts in human lymphoid cells. *J. Cell. Biochem.* 38: 117–126.
38. Zhang, D. J., Q. Wang, J. Wei, G. Baimukanova, F. Buchholz, A. F. Stewart, X. Mao, and N. Killeen. 2005. Selective expression of the Cre recombinase in late-stage thymocytes using the distal promoter of the Lck gene. *J. Immunol.* 174: 6725–6731.
39. Witczak, O., B. S. Skålhegg, G. Keryer, M. Bornens, K. Taskén, T. Jahnsen, and S. Ørstavik. 1999. Cloning and characterization of a cDNA encoding an A-kinase anchoring protein located in the centrosome, AKAP450. *EMBO J.* 18: 1858–1868.
40. Abrahamsen, H., G. Baillie, J. Ngai, T. Vang, K. Nika, A. Ruppelt, T. Mustelin, M. Zaccolo, M. Houslay, and K. Taskén. 2004. TCR- and CD28-mediated recruitment of phosphodiesterase 4 to lipid rafts potentiates TCR signaling. *J. Immunol.* 173: 4847–4858.
41. Lovatt, M., A. Filby, V. Parravicini, G. Werlen, E. Palmer, and R. Zamoyska. 2006. Lck regulates the threshold of activation in primary T cells, while both Lck and Fyn contribute to the magnitude of the extracellular signal-related kinase response. *Mol. Cell. Biol.* 26: 8655–8665.
42. Holmes, K. L., H. C. Morse, III, M. Makino, R. R. Hardy, and K. Hayakawa. 1990. A unique subset of normal murine CD4+ T cells lacking Thy-1 is expanded in a murine retrovirus-induced immunodeficiency syndrome, MAIDS. *Eur. J. Immunol.* 20: 2783–2787.
43. Moutschen, M. P., S. Colombi, M. Deprez, F. Van Wijk, C. Hotermans, M. T. Martin, R. Greimers, and J. Boniver. 1994. Population dynamics of CD4+ T cells lacking Thy-1 in murine retrovirus-induced immunodeficiency syndrome (MAIDS). *Scand. J. Immunol.* 39: 216–224.
44. de Leval, L., S. Colombi, S. Debrus, M. A. Demoitié, R. Greimers, P. Linsley, M. Moutschen, and J. Boniver. 1998. CD28-B7 costimulatory blockade by CTLA4Ig delays the development of retrovirus-induced murine AIDS. *J. Virol.* 72: 5285–5290.
45. Williams, R. O. 2002. Cutting edge: A-kinase anchor proteins are involved in maintaining resting T cells in an inactive state. *J. Immunol.* 168: 5392–5396.
46. Mosenden, R., and K. Taskén. 2011. Cyclic AMP-mediated immune regulation-Overview of mechanisms of action in T cells. *Cell Signal.* 23: 1009–1016.
47. Torheim, E. A., E. Jarnaess, B. Lygren, and K. Taskén. 2009. Design of proteolytically stable RI-anchoring disruptor peptidomimetics for in vivo studies of anchored type I protein kinase A-mediated signalling. *Biochem. J.* 424: 69–78.
48. Kandel, E. S., and N. Hay. 1999. The regulation and activities of the multifunctional serine/threonine kinase Akt/PKB. *Exp. Cell Res.* 253: 210–229.
49. Stern, J. B., and K. A. Smith. 1986. Interleukin-2 induction of T-cell G1 progression and c-myb expression. *Science* 233: 203–206.
50. Betz, M., and B. S. Fox. 1991. Prostaglandin E2 inhibits production of Th1 lymphokines but not of Th2 lymphokines. *J. Immunol.* 146: 108–113.
51. Haraguchi, S., R. A. Good, and N. K. Day. 1995. Immunosuppressive retroviral peptides: cAMP and cytokine patterns. *Immunol. Today* 16: 595–603.
52. Hilkens, C. M., A. Snijders, F. G. Snijdewint, E. A. Wierenga, and M. L. Kapsenberg. 1996. Modulation of T-cell cytokine secretion by accessory cell-derived products. *Eur. Respir. J. Suppl.* 22: 90s–94s.
53. Snijdewint, F. G., P. Kaliński, E. A. Wierenga, J. D. Bos, and M. L. Kapsenberg. 1993. Prostaglandin E2 differentially modulates cytokine secretion profiles of human T helper lymphocytes. *J. Immunol.* 150: 5321–5329.
54. Mahic, M., S. Yaqub, C. C. Johansson, K. Taskén, and E. M. Aandahl. 2006. FOXP3+CD4+CD25+ adaptive regulatory T cells express cyclooxygenase-2 and

suppress effector T cells by a prostaglandin E2-dependent mechanism. *J. Immunol.* 177: 246–254.
55. Deaglio, S., K. M. Dwyer, W. Gao, D. Friedman, A. Usheva, A. Erat, J. F. Chen, K. Enjyoji, J. Linden, M. Oukka, et al. 2007. Adenosine generation catalyzed by CD39 and CD73 expressed on regulatory T cells mediates immune suppression. *J. Exp. Med.* 204: 1257–1265.
56. Kobie, J. J., P. R. Shah, L. Yang, J. A. Rebhahn, D. J. Fowell, and T. R. Mosmann. 2006. T regulatory and primed uncommitted CD4 T cells express CD73, which suppresses effector CD4 T cells by converting 5′-adenosine monophosphate to adenosine. *J. Immunol.* 177: 6780–6786.
57. Bopp, T., C. Becker, M. Klein, S. Klein-Hessling, A. Palmetshofer, E. Serfling, V. Heib, M. Becker, J. Kubach, S. Schmitt, et al. 2007. Cyclic adenosine monophosphate is a key component of regulatory T cell-mediated suppression. *J. Exp. Med.* 204: 1303–1310.
58. Aukrust, P., E. M. Aandahl, B. S. Skålhegg, I. Nordøy, V. Hansson, K. Taskén, S. S. Frøland, and F. Müller. 1999. Increased activation of protein kinase A type I contributes to the T cell deficiency in common variable immunodeficiency. *J. Immunol.* 162: 1178–1185.
59. Mayrand, S. M., P. A. Healy, B. E. Torbett, and W. R. Green. 2000. Anti-Gag cytolytic T lymphocytes specific for an alternative translational reading frame-derived epitope and resistance versus susceptibility to retrovirus-induced murine AIDS in F(1) mice. *Virology* 272: 438–449.
60. Rabbi, M. F., L. al-Harthi, M. Saifuddin, and K. A. Roebuck. 1998. The cAMP-dependent protein kinase A and protein kinase C-beta pathways synergistically interact to activate HIV-1 transcription in latently infected cells of monocyte/macrophage lineage. *Virology* 245: 257–269.
61. Amella, C. A., B. Sherry, D. H. Shepp, and H. Schmidtmayerova. 2005. Macrophage inflammatory protein 1alpha inhibits postentry steps of human immunodeficiency virus type 1 infection via suppression of intracellular cyclic AMP. *J. Virol.* 79: 5625–5631.
62. Cartier, C., B. Hemonnot, B. Gay, M. Bardy, C. Sanchiz, C. Devaux, and L. Briant. 2003. Active cAMP-dependent protein kinase incorporated within highly purified HIV-1 particles is required for viral infectivity and interacts with viral capsid protein. *J. Biol. Chem.* 278: 35211–35219.
63. Barnitz, R. A., F. Wan, V. Tripuraneni, D. L. Bolton, and M. J. Lenardo. 2010. Protein kinase A phosphorylation activates Vpr-induced cell cycle arrest during human immunodeficiency virus type 1 infection. *J. Virol.* 84: 6410–6424.
64. Li, P. L., T. Wang, K. A. Buckley, A. L. Chenine, S. Popov, and R. M. Ruprecht. 2005. Phosphorylation of HIV Nef by cAMP-dependent protein kinase. *Virology* 331: 367–374.